Phase Equilibrium and Physical Properties for the Purification of Propylene Carbonate (PC) and γ-Butyrolactone (GBL)

Tobias Mathuni,[†] Jae-Ik Kim,[‡] and So-Jin Park*[,‡]

Department of Engineering Physics, University of Applied Sciences, Munich 80335, Federal Republic of Germany, and Department of Chemical Engineering, College of Engineering, Chungnam National University, Daejeon 305-764, Korea

The separation of propylene carbonate (PC) and γ-butyrolactone (GBL) from their primary impurities, which include water, propylene glycol (PG), and diethyl succinate (DES) and lower the potential of PC as a solvent in lithium batteries, was investigated. Consequently, the isobaric vapor−liquid equilibria (VLEs) for the PG + PC, GBL + DES, and water + GBL binary systems, as well as the solid−liquid equilibria (SLEs) for the GBL + DES and water + GBL binary systems, were characterized. The Wilson, nonrandom two-liquid (NRTL), and universal quasi-chemical (UNIQUAC) equations are used to describe the aforementioned VLEs and SLEs. Furthermore, we report the vapor pressures of PG, GBL, DES, and PC with a dynamic glass still from T = (376.99 to 485.91) K, as well as excess molar volume mixture properties (V^E), deviations in the molar refraction (ΔR), and deviations in viscosity ($\Delta\eta$) at 298.15 K for the same compositions.

Introduction

Propylene carbonate (PC) is frequently used as a high-permittivity component of electrolytes in lithium batteries, especially in combination with low-viscosity solvents. γ-Butyrolactone (GBL) is a preferable cosolvent for lithium ion batteries because of its good physical properties.[1,2] The increasing demand for portable and wireless electronic devices, such as portable phones, digital cameras, and notebook computers, has resulted in an increasing reliance on lithium ion batteries to power these electronic devices. Therefore, there is an increasing demand for secondary batteries that are lightweight, are small, and exhibit high energy densities. Lithium ion batteries exhibit high voltages and high energy densities but require high purity electrolyte solvents, which makes solvent separation and purification processes very important. The presence of trace impurities, such as water (<100 ppm), markedly affects the performance of lithium ion battery solvents.[3] PC can be directly synthesized from propylene glycol (PG) and CO_2 using different catalysts, such as modified zinc oxide. Recently, CeO_2-ZrO_2, Bu_2SnO, and $Bu_2Sn(Ome)_2$ have been developed to synthesize PC from PG and CO_2.[4] In addition, the alcoholysis of urea with PG to synthesize PC is an available approach to using PG.[5] As a result, PG is a major impurity of PC.[3] A system that is capable of more effective separation is required because the binary system PG + PC has an azeotropic character.[6]

To realize more effective separation, GBL is produced as a byproduct from the production of 1,4-butanol via the hydrogenation of the diethyl esters of maleic, fumaric, or succinic acid.[7] Diethyl succinate (DES) is an intermediate step in the synthesis of GBL, and furthermore, GBL can be directly hydrogenated from DES.[8−10] Consequently, DES is a possible impurity of GBL. Several patents have been established that outline the separation of GBL from a mixture that contains DES and other byproduct that derive from the vapor phase catalytic hydrogenation of the diethyl esters of maleic, fumaric, or succinic acid. Therein, "The isolation of pure GBL from said mixtures is not possible by normal distillation because GBL forms an azeotrope with DES"[7] and "...the recovery of pure GBL from the GBL rich fraction is problematic because diethyl succinate forms an azeotrope with GBL and co distils therewith."[11] Patent EP-A 256,813 proposes that the DES should be separated from such mixtures that contain GBL via extraction using an organic solvent. The resultant extract, which consists of DES and an organic solvent, is subsequently extracted using a polar solvent, such as water.[7] EP-A 255,400 describes a method of producing pure GBL, wherein the problem of azeotrope formation by GBL + DES is avoided by the addition of diethyl maleate; however, the separation of the products from the hydrogenation of maleic, fumaric, or succinic acid is problematic because GBL + DES forms an azeotropic system.

This paper is a part of a systematic research study that intends to develop purification methods for PC and GBL, which are important lithium ion battery electrolyte solvents. The development of purification methods for these solvents is important because the demands for highly purified battery solvents and higher density batteries are increasing. Primary solvent impurities, such as water, and impurities that are challenging to remove from the solvents are investigated in this research. Aside from a common distillation process, the feasibility of using crystallization for solvent purification has also been studied. In order to investigate these distillation and crystallization processes, the isobaric vapor−liquid equilibria (VLEs) and solid−liquid equilibria (SLEs) for the aforementioned solvent systems were measured over the whole compositional ranges. In order to establish a better understanding of the aforementioned solvent systems and establish mixture data, excess properties, such as the excess molar volume (V^E), deviations in refraction (ΔR), and deviations in viscosity ($\Delta\eta$), were measured.[12]

The separation of PC from PG via distillation is of strategic interest because they form an azeotrope at low pressures. In order to verify that the azeotrope disappears at a pressure of

* Corresponding author. Tel.: +82-42-821-5684. Fax: +82-42-823-6414. E-mail: sjpark@cnu.ac.kr.
[†] University of Applied Sciences.
[‡] Chungnam National University.

10.1021/je100803e
Published on Web 12/15/2010

Table 1. CAS Number, Purity, Water Content, and Physical Properties of PC, GBL, PG, DES, and Water

				ρ				η		
				g·cm^{-3} at 298.15 K		n_D at 298.15 K		mPa·s at 298.15 K		$\Delta_{fus}H$
Compound	CAS number	wt % by G.C.	$1/10^6$ w_{H_2O}	present study	lit. value	present study	lit. value	present study	lit. value	J·mol^{-1}
PC	108-32-7	>99.9	9.8	1.19944	1.1988[13]	1.4198	1.4210[13]	2.389	2.4711[17]	
DES	123-25-1	>99.9	27	1.03553	1.0353[16]	1.4179	1.4196[16]	2.393		51320.000[24]
GBL	96-48-0	>99.9	37	1.12454	1.1239[14]	1.4350	1.4346[14]	1.654	1.6529[18]	9564.601[24]
PG	57-55-6	>99.9	70.1	1.03165	1.0327[15]	1.4313	1.4324[15]	44.445		
water	7732-18-5	>99.9		0.99711	0.9970[15]	1.33249	1.3325[15]	0.876	0.8903[19]	5996.100[24]

11.0 kPa, the isobaric VLE of PG + PC was measured at 12.0 kPa. Unfortunately, purification by crystallization for the same system is not feasible because PC and PG have similar melting points. Furthermore, the separation of water + PC is also less interesting because water is only partially miscible in PC. Accordingly, the isobaric VLE of PG + PC and its excess properties were analyzed in detail.

Even though GBL has an azeotrope with DES,[7,11] water is the primary impurity in GBL and markedly affects the performance of lithium ion batteries.[3] Accordingly, the isobaric VLEs, SLEs, and excess properties of GBL + DES and water + GBL were closely analyzed. Following the measurement of the isobaric VLE of PG + PC at 12.0 kPa, the isobaric VLEs of GBL + DES and water + GBL were measured at the same pressure so as to provide uniform results.

Experimental Section

Materials. All of the chemicals that were used in this study were purchased from commercial sources. PC and GBL were obtained with over 99.5 wt % and 99.0 wt % purities, respectively, from Samchum Chemicals. PG was obtained with over 98.0 wt % purity from Junsei Chemical. DES was obtained with over 99.0 wt % purity from Tokyo Kasei Industry Co. Ltd. After carefully drying with Union Carbide 3-Å molecular sieves (from Fluka), the microwater content for each chemical was measured. The purities of the chemicals were characterized with an Agilent gas chromatographer 6890 using the Karl Fischer method and a 684 KF coulometer from Metrolm, wherein measured densities, refractive indices, and viscosities were compared to those from the literature. The purities of the chemicals exceeded 99.9 wt % according to gas chromatography, wherein no significant impurities were detected. Table 1 lists the measured and referenced[13−19] densities (ρ), refractive indices (n_D), viscosities (η), and heats of fusion (Δh_{fus}) for the pure components. The water used in this study was obtained at a purity in excess of 99.9 wt % from J. T. Baker, which was also verified by gas chromatography by comparing measured densities, refractive indices, and viscosities to those in the literature.

Apparatus and Procedure. A Dr. Sieg & Röck-type recirculating glass still was used for the vapor pressure and isobaric VLEs measurements. The pressure of the still was controlled with a Baratron pressure regulating system, which had an uncertainty of ± 0.1 kPa. The equilibrium temperature was measured with a Pt-100 temperature probe (with an uncertainty of ± 0.01 K). The liquid and vapor samples were analyzed using a gas chromatograph (HP 6890N, U.S.A.) with an HP-5 (30 m × 0.32 mm × 0.25 μm) capillary column and a thermal conductivity detector. The calibration curve has been constructed for whole composition range with known injection amount of standard sample mixtures of the binary systems. The mole fraction of the liquid and vapor samples were directly determined from the integrated chromatogram.

Antoine coefficients were determined using the same apparatus that was used for the isobaric VLEs measurements. At several different pressures, pure liquid was heated in a flask until boiling. If, after 20 min, there was no observable change in temperature, the boiling temperature was recorded. Measuring was started with the smallest good adjustable pressure of 4 kPa. The experimental procedure for VLEs is described and verified in detail elsewhere.[20]

Mixture samples were prepared in ca. 20-mL vials by mass using a microbalance (A & D, HA202) with a precision of ± 1 · 10^{-5} g, charging the higher-boiling component first to minimize vaporization effects. The uncertainty in the mole fraction of the mixture sample was less than ± 1 · 10^{-4}.

SLEs were determined at atmospheric pressure using a triple-jacket glass tube, wherein the melting process can be visually observed. The measurement equipment and techniques have been previously described.[12] The temperature was determined with a digital thermometer (ASL F250, U.K.). First, the superficial melting point of given compositions was determined when the last crystal was disappeared. And then, cryostat medium temperature was regulated as the same temperature of the superficial melting point, the true melting point was carefully determined by the same determining process. The uncertainty of the melting temperature was determined to be ± 0.02 K and estimated uncertainty of mole fraction was less than ± 1 · 10^{-4}.

The densities of the solutions and pure components were measured at 298.15 K and atmospheric pressure using an Anton Paar DMA-5000 vibrating tube. The densimeter was calibrated with water and dried air. The manufacturer stated uncertainty of the densimeter was less than ± 5 · 10^{-6} g cm^{-3} within the range of (0 to 3) g cm^{-3}, and the temperature accuracy was ± 0.01 K. The measurements were performed in triplicate at each mole fraction, and the results were averaged.

The refractive indices of the solutions and pure components were measured at 298.15 K and atmospheric pressure using a digital refractometer (KEM, model RA-520N, Japan). According to the manufacturer, the uncertainty of this refractometer is ± 5 · 10^{-5} from 1.32 to 1.40 and ± 1 · 10^{-4} from 1.40 to 1.58. The uncertainty of the temperature was ± 5 · 10^{-2} K. The measurements were performed in triplicate at each mole fraction, and the results were averaged.

The kinematic viscosities of the solutions were measured using an Ubbelohde viscometer (Schott, Germany) and an automatic measuring unit (LAUDA, model PVS1) at 298.15 K and atmospheric pressure. The Ubbelohde viscometer was mounted in a water thermostat bath. The temperature of the water bath was determined using a digital thermometer (ASL F250, U.K.) at an uncertainty of ± 0.02 K. The uncertainty of the flowing time measurement was ± 0.01 s. The uncertainty in the viscometer measurement is ± 0.1%. The measurements were performed in triplicate at each mole fraction, and the results were averaged.

Theory. To determine the VLE a simplified VLE equation (modified Raoult's law) were used.

$$y_i P = x_i \gamma_i P_i^S \tag{1}$$

Table 2. Experimental Vapor Pressures of PC, DES, GBL, and PG

pressure	PC	DES	GBL	PG
P^{Sat}	T	T	T	T
kPa	K	K	K	K
4.0	407.97	392.46	376.99	378.00
10.0	432.45	417.39	400.58	398.24
12.0	437.77	423.15	405.68	402.54
20.0	453.60	437.53	420.76	415.13
30.0	467.23	453.15	433.66	425.72
40.0	477.53	462.10	443.36	433.59
50.0	485.91	467.78	451.22	439.90
60.0			457.88	445.20
70.0			463.68	449.79
80.0			468.84	453.84
90.0			473.49	457.48
100.0			477.54	460.79

The activity coefficients of the components in the liquid phase were calculated as follows:

$$y_i\varphi_i^{V}P = x_i y_i P_i^{S}\varphi_i^{S}\exp\left\{\frac{V_i^{L}(P - P_i^{S})}{RT}\right\} \quad (2)$$

where P is the total pressure, γ_i is the mole fraction of component i in the vapor phase, x_i is the mole fraction of component i in the liquid-phase, R is the gas constant, T is the temperature, P_i^{S} is the vapor pressure of pure component i, V_i^{L} is the liquid molar volume of pure component i, φ_i^{V} and φ_i^{S} are the fugacity coefficients of component i in the mixture vapor phase and in the pure state, respectively, and γ_i is the activity coefficient of component i.

the Antoine equation were used.

$$\log P^{S}/\mathrm{kPa} = \mathrm{A} - \frac{\mathrm{B}}{\mathrm{C} + T/\mathrm{K}} \quad (3)$$

The mean deviation of the mole fraction in the vapor phase (Δy) was calculated with the following equation:

$$\Delta y = \frac{1}{n}\sum_{n}(y - y_{cal}) \quad (4)$$

where n is the number of measured points, y is the experimentally determined mole fraction of the vapor phase, and y_{cal} is the calculated mole fraction of the vapor phase. In order to calculate the Antoine coefficients, the experimental data were fitted to the Antoine equation. The standard deviation (σ_{st}) of the correlation is defined as[21]

$$\sigma_{st} = \left[\frac{\sum_{i}(P_{cal}^{S} - P^{S})_i^{2}}{(n - N)}\right]^{1/2} \quad (5)$$

where P_{cal}^{S} is the Antoine equation-calculated saturation vapor pressure, P^{S} is the experimental saturation vapor pressure, n is

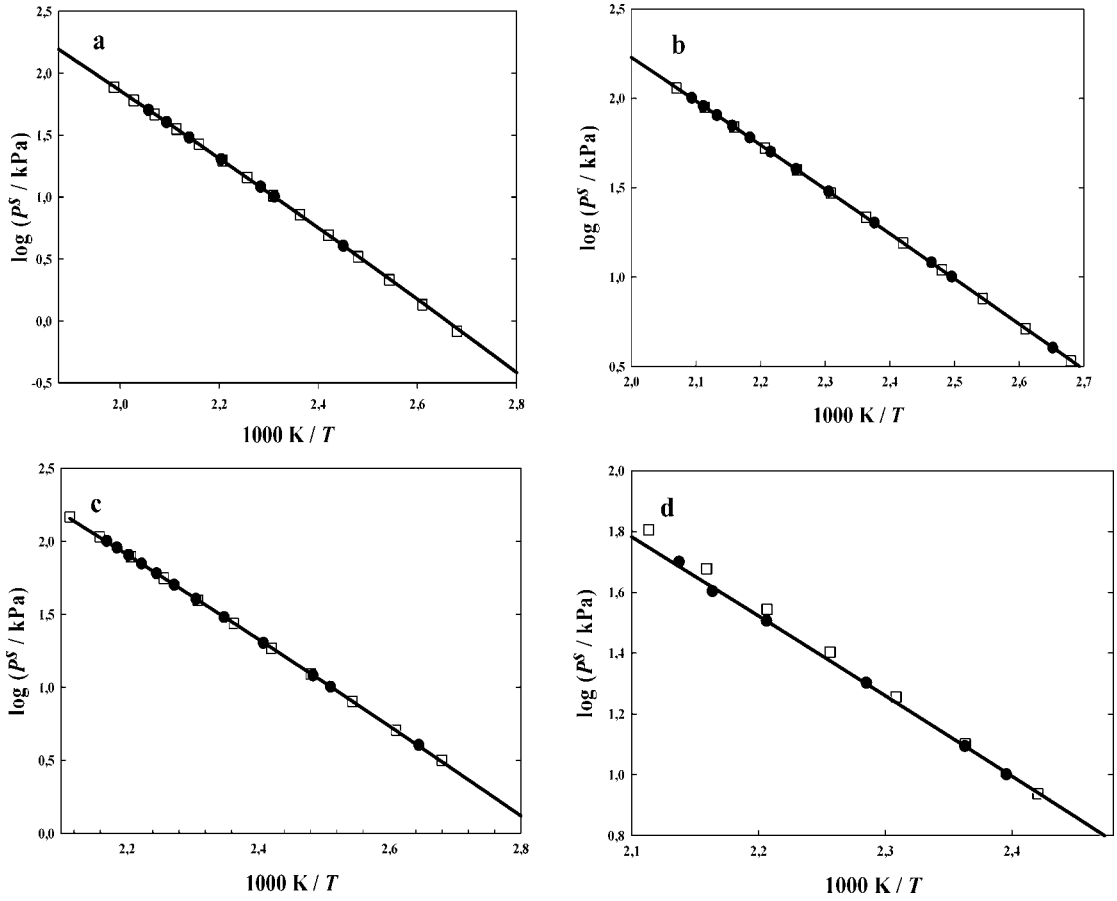

Figure 1. Vapor pressures with logarithmically plotted pressure on the ordinate and linear inverse temperature plotted across the abscissa. (a), PC; (b), GBL; (c), PG; (d), DES; ●, experimental vapor pressures; □, vapor pressures calculated by Antoine constants from DDB. Solid lines were calculated from Antoine equation.

Table 3. Antoine Constants Calculated in kPa and K as well as Standard Deviation for the Fitted Vapor Pressures of PC, DES, GBL, and PG[a]

component	A	B	C	σ_{st} / kPa
PC	9.65148	2127.589	−56.098	0.06666
DES	9.70612	2126.438	−44.311	0.79993
GBL	9.77809	2125.674	−32.724	0.10666
PG	10.3363	2128.187	−62.280	0.35997

[a] $\sigma_{st} = [(\sum_i (p^S_{cal} - p^S)_i^2)/(n - N)]^{1/2}$ where n is the number of experimental data and N is the number of the fitted parameters.

the number of experimental data, and N is the number of the fitted parameters. In this case, there are three fitted parameters.

The SLE determination have previously been characterized.[12] The binary V^E, ΔR, and $\Delta\eta$ data correlated well with a four-parameter Redlich−Kister polynomial equation of the following form:[22,23]

$$M^E = x_1 x_2 \sum_{i=1}^{n} A_i (x_1 - x_2)^{i-1} \quad (6)$$

where A_i are adjustable parameters.

Results and Discussion

Antoine Equation. The vapor pressures of the pure chemicals were evaluated via boiling temperature measurements at different fixed pressures. The temperatures and pressures were measured from (376.99 to 460.79) K and from (4 to 100) kPa for GBL and PG, as well as from (392.46 to 485.91) K and from (4 to 50) kPa for PC and DES. The results of these measurements are summarized in Table 2. The experimental vapor pressure data were fitted to the Antoine equation (q.v. eq 2). Figure 1 plots experimental data points (circle) using logarithmically plotted pressure on the ordinate and linear temperature plotted across the abscissa. The solid line represents the correlated Antoine equation, whereas the square symbols represent the vapor pressures that were calculated using Antoine constants from the Dortmund Data Bank.[24] The Antoine constants and the standard deviations of the fitted vapor pressures are listed in Table 3. The experimental data agree well with those from the literature, and the Antoine coefficient can be used in the aforementioned experimental temperature ranges.

Isobaric Vapor−Liquid Equilibrium. The experimental isobaric VLE data of PG + PC, GBL + DES, and water + GBL of the liquid and vapor phases are listed together with their boiling points in Table 4. According to these data, the last measured point of PG + PC is already azeotropic. GBL + DES and water + GBL do not have azeotropic points. Activity coefficients were correlated using the common G^E models (Wilson, NRTL, and UNIQUAC). The parameters A_{ij} for the Wilson, NRTL, and UNIQUAC equations are expressed as

$$\text{Wilson} \qquad A_{ij} = \lambda_{ij} - \lambda_{ii}/\text{J·mol}^{-1} \quad (7)$$

$$\text{NRTL} \qquad A_{ij} = g_{ij} - g_{ii}/\text{J·mol}^{-1} \quad (8)$$

$$\text{UNIQUAC} \qquad A_{ij} = u_{ij} - u_{ii}/\text{J·mol}^{-1} \quad (9)$$

Table 5 depicts the best-fit model parameters and mean deviations of the vapor phase mole fractions of PG + PC, GBL + DES, and water + GBL. As can be observed from the mean deviations, in all cases, the experimental data agree well with the calculated values. Figure 2 depicts the experimental data of the three systems. The solid line represents the fitted G^E model

Table 4. Experimental Isobaric VLE Data for the Systems of PG + PC, GBL + DES, and Water + GBL at 12 kPa

T_b / K	x_1	y_1	T_b / K	x_1	y_1	T_b / K	x_1	y_1
PG (1) + PC (2)								
432.77	0.0143	0.1671	408.03	0.3208	0.7318	403.01	0.7448	0.8626
425.17	0.0575	0.3739	405.52	0.4427	0.7873	402.85	0.7677	0.8733
419.53	0.0967	0.5041	404.97	0.5173	0.8097	402.48	0.8475	0.8952
417.63	0.1157	0.5385	404.35	0.5863	0.8214	402.20	0.9445	0.9490
415.49	0.1428	0.5920	403.87	0.6221	0.8319	402.19	0.9660	0.9682
411.49	0.2216	0.6716	403.28	0.6908	0.8482	402.38	0.9831	0.9817
GBL (1) + DES (2)								
419.90	0.0415	0.0989	410.79	0.4263	0.5885	405.88	0.9456	0.9540
418.48	0.0667	0.1724	410.17	0.4682	0.6184	405.75	0.9625	0.9689
417.31	0.1138	0.2356	409.16	0.5126	0.6744	405.86	0.9759	0.9784
415.96	0.1560	0.3039	408.62	0.5742	0.7000	405.55	0.9841	0.9860
414.97	0.2200	0.3818	407.95	0.6502	0.7522	405.60	0.9918	0.9927
413.38	0.2801	0.4539	407.01	0.7497	0.8207	405.66	0.9963	0.9967
412.31	0.3368	0.5082	406.28	0.8438	0.8808			
411.66	0.3829	0.5509	405.95	0.8953	0.9177			
Water (1) + GBL (2)								
397.82	0.0107	0.2469	330.09	0.3722	0.9775	324.58	0.8017	0.9870
386.50	0.0159	0.5474	328.38	0.4717	0.9805	324.31	0.8383	0.9878
365.13	0.0567	0.8094	327.46	0.5209	0.9822	324.00	0.8911	0.9895
356.23	0.0898	0.9032	326.53	0.5892	0.9837	323.05	0.9839	0.9959
346.37	0.1533	0.9439	325.95	0.6680	0.9847	323.38	0.9618	0.9932
337.05	0.2073	0.9635	325.15	0.7319	0.9857			
333.85	0.2682	0.9632	324.79	0.7697	0.9865			

Table 5. Best Fit G^E Model Parameters of the Isobaric VLE Data for the Systems of PG + PC, GBL + DES, and Water + GBL and the Corresponding Mean Deviations of the Vapor Phase Mole Fraction at 12 kPa

system	G^E model	A_{12} / J·mol^{-1}	A_{21} / J·mol^{-1}	α_{12}	Δy_1
PG (1) + PC (2)	NRTL	3729.24	2192.88	0.6	0.0091
GBL (1) + DES (2)	NRTL	1454.13	222.94	0.3	0.0050
water (1) + GBL (2)	Wilson	4351.63	1773.32		0.0134

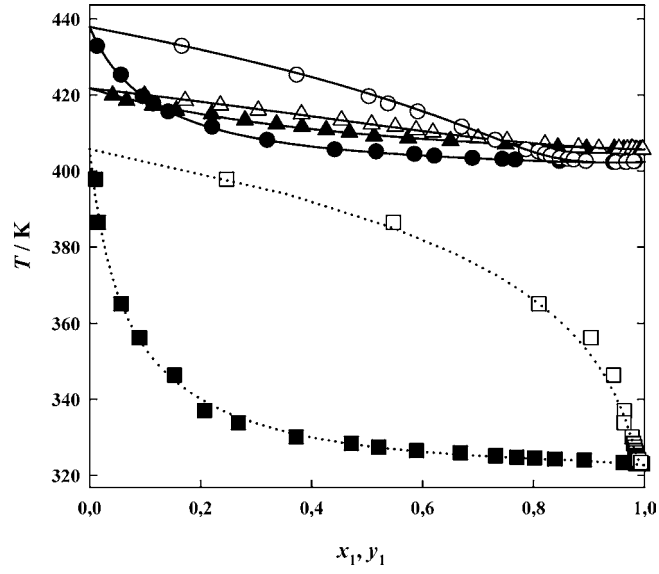

Figure 2. $T/x-y$ diagram of the isobaric VLE systems at 12 kPa. filled symbols, liquid phase; open symbols, vapor phase; ●, PG (1) + PC (2); ▲, GBL (1) + DES (2); □, water (1) + GBL (2). Solid lines were calculated from g^E model equation (Table 5).

Table 6. Correlated Possible Azeotropic Point Areas of the System of PG (1) + PC (2) for Several G^E Models

G^E model	x_1	T_b / K
NRTL	0.9441	402.24
Wilson	0.9459	402.25
UNIQUAC	0.9533	402.32

Table 7. Mixture Composition in Mole Fraction for the Liquid and Vapor Phases at Different Pressures Together with the Boiling Point for the System of PG (1) + PC (2)

P / kPa	T_b / K	x_1	y_1
12.0	402.38	0.9831	0.9817
13.0	404.32	0.9821	0.9821
14.0	406.07	0.9821	0.9826

Table 8. Experimental SLE Data for the Systems of GBL + DES and Water + GBL at Atmospheric Pressure

system	x_1	T / K	x_1	T / K
GBL (1) + DES (2)	0.0000	251.63	0.7800	210.08
	0.0501	250.97	0.8000	210.45
	0.3000	243.01	0.8400	215.95
	0.4000	238.51	0.8700	220.09
	0.5000	232.06	0.9000	223.05
	0.6000	225.76	0.9500	227.65
	0.7000	218.05	1.0000	229.43
water (1) + GBL (2)	0.0000	229.43	0.4000	248.55
	0.0502	227.89	0.5000	252.39
	0.1000	226.31	0.6000	256.39
	0.1301	225.39	0.7000	259.24
	0.1600	225.16	0.8000	262.11
	0.1800	228.86	0.8992	265.99
	0.2000	232.25	0.9498	269.18
	0.3000	241.47	1.0000	273.05

with the best accuracy. According to Figure 2, the PG + PC system presents positive deviations from ideality and is a minimum boiling azeotrope at 12 kPa. GBL + DES and water + GBL do not show azeotropic behaviors. Table 6 depicts the azeotropic mole fraction and boiling temperature, according to the G^E models, for PG + PC. The azeotropic mole fraction of PG + PC was evaluated at different pressures because the literature say that there is no azeotrope at 12 kPa.[6] Table 7 depicts a shift in the azeotropic point as a function of changing pressure, wherein it can be observed that a pressure in excess of 14 kPa nearly quenches the azeotropic character.

For GBL + DES, the calculation of VLE by all three G^E models demonstrated that there was no azeotropy over the entire compositional range of GBL + DES at 12 kPa; however, in this system, GBL + DES have similar boiling points, which complicates separation distillation because the distillation column will require a large number of stages.

For the GBL + water system, it is evident from the graphs that the system does not exhibit azeotropic behavior and appreciably deviate from Raoult's law. The purification of GBL from water should be easy via distillation at 12 kPa.

Solid−Liquid Equilibrium. Table 8 depicts the experimental SLE data for the binary systems of GBL + DES and water + GBL. The heats of fusion and melting points of the pure substances are required to describe the SLEs. In addition, Table 9 summarizes the best-calculated G^E model parameters of the systems. Correspondingly, Figure 3 depicts the plotted experimental data together with correlated values that were obtained from the best-fit model as solid line in a *T/x* diagram. Eutectic behavior is assumed for the GBL + DES and water + GBL system. For the GBL + DES system, the interpolated eutectic point that was calculated by the UNIQUAC equation was recorded for a GBL mole fraction of 0.7808 at 209.90 K. For the water + GBL system, the interpolated eutectic point that was calculated by the Wilson equation is recorded for a mole fraction of 0.1504 at 224.60 K. Thus, the corresponding best-fit interpolated eutectic points for the GBL + DES and water + GBL systems are listed in Table 10.

Table 9. Best Fit G^E Model Parameters of the SLE Data for the Systems of GBL + DES and Water + GBL as well as the Corresponding RMSD Value at Atmospheric Pressure

system	G^E model	A_{12} / J·mol^{-1}	A_{21} / J·mol^{-1}	rmsd T / K
GBL (1) + DES (2)	UNIQUAC	−2826.1581	2391.3526	0.82
water (1) + GBL (2)	Wilson	4767.0404	545.3844	0.37

Table 10. Correlated Eutectic Points of the Systems of GBL + DES and Water (1) + GBL (2) for the Best Fitted G^E Model

system	G^E model	x_1^L	T / K
GBL (1) + DES (2)	UNIQUAC	0.7808	209.90
water (1) + GBL (2)	Wilson	0.1504	224.60

Physical Excess Properties. The experimental values for density, refractive index, and viscosity of the PG + PC, GBL + DES, and water + GBL systems at several different mole fractions were measured at 298.15 K and are listed together with the calculated V^E, ΔR, and $\Delta\eta$ in Table 11. The fitted parameters of the Redlich−Kister equation for the excess properties are listed together with the standard deviations of

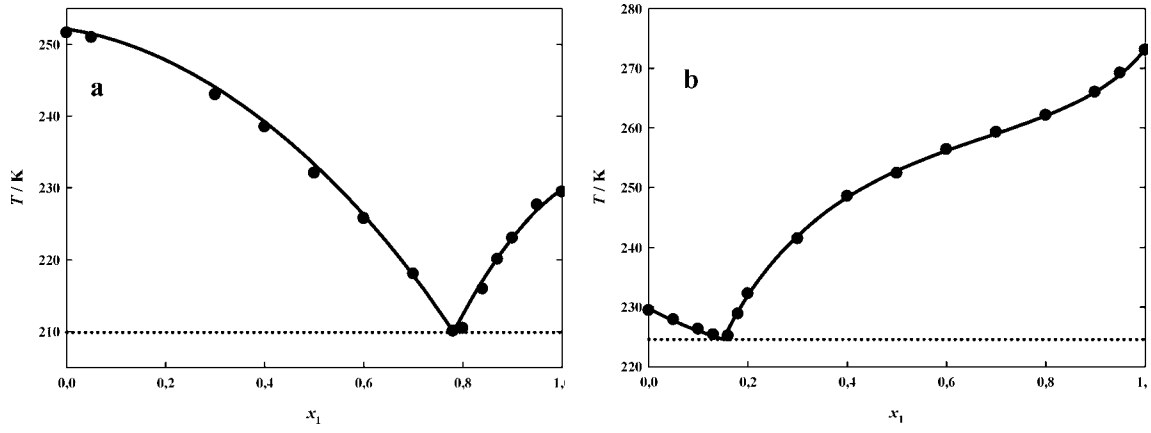

Figure 3. *T/x* diagrams of the SLE systems at atmospheric pressure. (a) GBL (1) + DES (2); (b) water (1) + GBL (2); ●, experimental data. Solid lines were calculated from g^E model equation (Table 9).

Table 11. Density, Excess Molar Volume, Refractive Index, Deviations in Molar Refractivity, Viscosity, and Deviations in Viscosity of the Systems of PG + PC, GBL + DES, and Water + GBL Measured at 298.15 K

system	x_1	ρ / g·cm^{-3}	V^E / cm^3·mol^{-1}	n_D	ΔR	η / mPa·s	$\Delta\eta$ / mPa·s
PG (1) + PC (2)	0.0000	1.1994	0.0000	1.4198	0.0000	2.390	0.000
	0.0500	1.1909	0.0873	1.4199	−0.0139	2.436	−2.056
	0.1000	1.1824	0.1590	1.4199	−0.0325	2.533	−4.061
	0.2000	1.1664	0.2234	1.4207	−0.0557	2.921	−7.880
	0.3000	1.1502	0.2667	1.4213	−0.0850	3.550	−11.457
	0.4000	1.1342	0.2702	1.4223	−0.1042	4.758	−14.453
	0.5000	1.1179	0.2623	1.4235	−0.1080	6.071	−17.346
	0.6000	1.1016	0.2153	1.4249	−0.1072	8.461	−19.162
	0.7000	1.0851	0.1502	1.4264	−0.1026	11.817	−20.012
	0.8000	1.0680	0.0855	1.4278	−0.0922	17.375	−18.660
	0.9000	1.0506	0.0086	1.4294	−0.0665	27.535	−12.705
	0.9500	1.0414	−0.0115	1.4305	−0.0351	35.661	−6.681
	1.0000	1.0316	0.0000	1.4313	0.0000	44.445	0.000
GBL (1) + DES (2)	0.0000	1.0355	0.0000	1.4179	0.0000	2.393	0.000
	0.0500	1.0375	0.0177	1.4185	−0.7723	2.381	0.029
	0.1000	1.0400	−0.0284	1.4190	−1.5370	2.375	0.056
	0.2000	1.0453	−0.0971	1.4201	−2.9219	2.356	0.107
	0.2999	1.0511	−0.1404	1.4213	−4.0903	2.319	0.151
	0.4000	1.0578	−0.1928	1.4227	−5.0068	2.284	0.184
	0.5000	1.0653	−0.2218	1.4242	−5.6107	2.226	0.204
	0.6000	1.0738	−0.2276	1.4259	−5.8220	2.153	0.207
	0.7000	1.0835	−0.2044	1.4278	−5.5397	2.073	0.191
	0.8000	1.0949	−0.1663	1.4299	−4.6296	1.952	0.153
	0.9000	1.1084	−0.1025	1.4323	−2.8833	1.817	0.090
	0.9500	1.1162	−0.0643	1.4336	−1.6113	1.745	0.049
	1.0000	1.1245	0.0000	1.4350	0.0000	1.654	0.000
water (1) + GBL (2)	0.0000	1.1245	0.0000	1.4350	0.0000	1.654	0.000
	0.0500	1.1230	0.0018	1.4337	−0.8063	1.621	0.006
	0.1002	1.1215	−0.0136	1.4325	−1.5946	1.600	0.024
	0.2000	1.1182	−0.0438	1.4295	−3.0892	1.606	0.108
	0.3000	1.1151	−0.1219	1.4265	−4.4543	1.645	0.225
	0.4000	1.1109	−0.1763	1.4226	−5.6518	1.706	0.363
	0.5000	1.1059	−0.2447	1.4175	−6.6238	1.766	0.501
	0.6000	1.0988	−0.2863	1.4116	−7.2398	1.801	0.614
	0.7000	1.0886	−0.3059	1.4017	−7.3964	1.787	0.678
	0.8000	1.0732	−0.2909	1.3888	−6.7408	1.668	0.637
	0.9000	1.0471	−0.2110	1.3684	−4.7163	1.385	0.056
	0.9500	1.0266	−0.1276	1.3531	−2.8366	1.160	0.025
	1.0000	0.9971	0.0000	1.3325	0.0000	0.876	0.000

Table 12. Fitted Parameters of the Redlich−Kister Polynomial Equation and Corresponding Standard Deviations for the Physical Excess Properties of the Systems of PG (1) + PC (2), GBL (1) + DES (2), and Water (1) + GBL (2) at 298.15 K

excess property	system	A_1	A_2	A_3	A_4	σ_{st}
V^E/cm^3·mol^{-1}	PG + PC	1.0295	−0.5233	−0.1951	−0.7466	0.0058
	GBL + DES	−0.8854	−0.2492	0.2776	−0.5231	0.0105
	water + GBL	−0.9549	−1.0605	−0.3748	−0.5321	0.0064
ΔR	PG + PC	−0.4306	−0.0662	−0.1288	−0.2737	0.0031
	GBL + DES	−22.4256	−8.3504	−3.2781	−1.6172	0.0057
	water + GBL	−26.2703	−15.9615	−13.2427	−9.0433	0.0574
$\Delta\eta$/mPa·s	PG + PC	−68.7445	−48.1390	−39.4194	− 20.6495	0.0994
	GBL + DES	0.8153	0.2426	−0.0007	−0.0085	0.0047
	water + GBL	2.0021	2.6211	0.9025	0.3929	0.0018

the binary systems in Table 12. The correlated values agree well with the experimental data.

The experimental V^E at 298.15 K for the PC + PG, GBL + DES, and water + GBL binary systems are shown together in Figure 4. Due to the almost negative volume deviation from ideal mixing, it can be concluded that there is a remarkable molecular interaction between GBL + DES and water + GBL. The PG + PC system exhibits an almost positive deviation, which means there is no observed interaction between the two components. These results can be discussed in terms of several phenomena that may simply be separable into dispersion forces, dipole−dipole interactions, and large differences in molar volumes. The positive V^E values may be attributed to the contribution of dispersion forces between the PG and PC molecules. Apparently, a small amount of PC in PG causes a small interaction. However, the dispersion forces grow as a function of the PC mole fraction until they peak inside the PC-rich phase. On the other hand, the negative V^E values of the GBL + DES system may be attributed to dipole−dipole interactions between GBL and DES molecules. Because of its large dipole moment ($\mu = 4.12$ D),[25] GBL can strongly interact with DES through dipole−dipole interactions in the mixtures, which negatively contribute to V^E. Thus, it may be concluded that dipole−dipole interactions between unlike molecules are primarily responsible for the negative values of V^E in the binary system. For a small amount of GBL in DES, there is no obvious interaction; however, as the GBL concentration is increased in this mixture, the dipole−dipole interactions therein increase and peak near the GBL rich phase. The interaction of water + GBL strongly depends on the amount of GBL. A small mole fraction of GBL causes strong contractions in this binary system; however, a small mole fraction of water in GBL initially exhibits

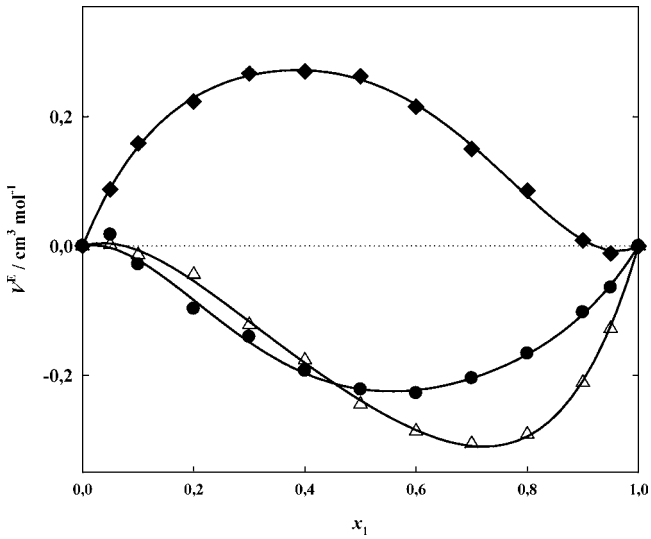

Figure 4. Plotted excess molar volumes V^E of the binary systems at 298.15 K. ◆, PG (1) + PC (2); ●, GBL (1) + DES (2); △, water (1) + GBL (2). Solid lines were calculated from Redlich−Kister parameters (Table 12).

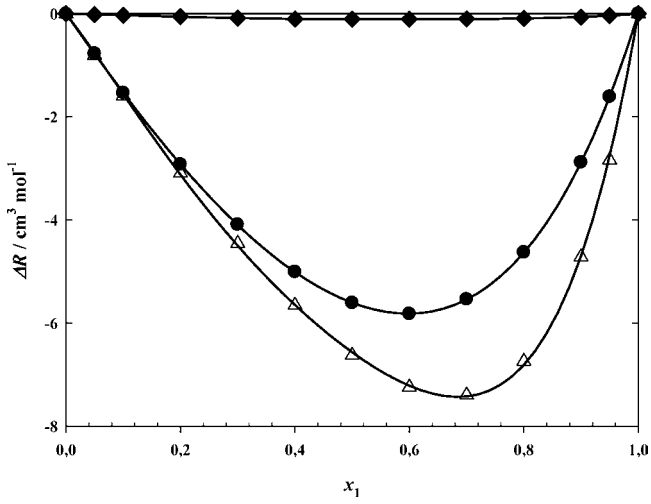

Figure 5. Plotted deviations in molar refractivities ΔR of the binary systems at 298.15 K. ◆, PG (1) + PC (2); ●, GBL (1) + DES (2); △, water (1) + GBL (2). Solid lines were calculated from Redlich−Kister parameters (Table 12).

no observable interaction and then later a slow swelling. The large differences in the molar volumes of the pure components are possible causes of this behavior. In order to change the mole fraction in the water rich phase, a large amount of GBL is necessary. Structure contributions can arise from the geometrical fitting of one component into the other. Differences in the molar volume and free volume between components can lead to negative contributions of V^E.

Variations of ΔR as a function of mole fraction for the PG + PC, GBL + DES, and water + GBL systems at 298.15 K are graphically depicted in Figure 5 with the calculated solid lines using correlated Redlich−Kister parameters. Figure 5 demonstrates that ΔR negatively deviates from ideality over the entire compositional range for all three systems. These results agree well with the results of the V^E measurements. The PG + PC system exhibits almost no deviation; hence, there is no obvious interaction. The GBL + DES and water + GBL systems exhibit maximum deviations in ΔR at nearly the same mole fraction as that corresponding to a maximum deviation in V^E.

Figure 6 plots the $\Delta\eta$'s of PG + PC, GBL + DES, and water + GBL together with the calculated values using fitted

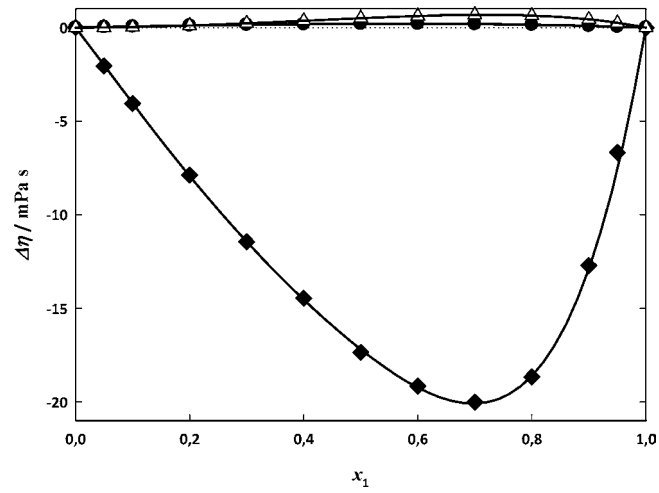

Figure 6. Plotted deviations in viscosities $\Delta\eta$ of the binary systems at 298.15 K. ◆, PG (1) + PC (2); ●, GBL (1) + DES (2); △, water (1) + GBL (2). Solid lines were calculated from Redlich−Kister parameters (Table 12).

Redlich−Kister parameters. The GBL + DES and water + GBL systems exhibit normal positive deviations from the ideal viscosity. In addition, according to Figure 6, the PG + PC system strongly and negatively deviates from the ideal viscosity. The viscosity of the PG + PC system is high because the highly viscous PG is a component of this system. From these data, it can be observed that systems with negative deviations in V^E have positive deviations in $\Delta\eta$ and vice versa. This phenomenon has already been reported in earlier literature and is confirmed here.[26] Other studies have already reported that systems with dispersion forces typically exhibit negative viscosity deviations.[27]

Conclusion

Vapor pressures for PC, GBL, PG, and DES were identified at temperatures ranging from (376.99 to 485.91) K. At low pressures, these observed vapor pressures agree well with those obtained using the Antoine equation. Isobaric VLE data for the binary mixtures, PG + PC, GBL + DES, and water + GBL were measured at 12 kPa in a Dr. Sieg & Röck-type recirculating glass still. The PG + PC binary system presents a minimum temperature azeotrope, and this azeotropic character appears to disappear at pressures in excess of 14 kPa. The GBL + DES binary system does not exhibit an azeotropic point at 12 kPa. The water + GBL system does not show azeotropic behavior and relatively large positive deviations from Raoult's law. SLE data for the GBL + DES and water + GBL binary systems were visually measured at atmospheric pressure and at temperature ranges of (210.08 to 251.63) K and (225.16 to 273.05) K, respectively. For both systems, eutectic behaviors are assumed. V^E, ΔR, and $\Delta\eta$ were determined for the PG + PC, GBL + DES, and water + GBL systems at 298.15 K and atmospheric pressure, which correlated well with the Redlich−Kister equation.

Literature Cited

(1) Bantu, N. R.; Bhatt, A. C.; Keesler, R. W.; Papathomas, K.; Sinclair, T. D.; Wagner, J. J. Propylene Carbonate Recovery Process. U.S. Patent 5281723, 1994.

(2) Lanz, M.; Novák, P. DEMS study of gas evolution at thick graphite electrodes for lithium-ion batteries: the effect of γ-butyrolactone. *J. Power Sources* **2001**, *102*, 277–282.

(3) Jasinski, R. J.; Kirkland, S. Analysis and Destillation of Propylene Carbonate. *Anal. Chem.* **1967**, *39*, 1663–1665.

(4) Bocksetette, M.; Wöhrle, D. W.; Braun, I.; Ekloff, G. S. Conventional and microwave-assisted crystallization inclusion of substituted rhodamine derivatives in AlPO4−5. *Microporous Mesoporous Mater.* **1998**, *23*, 83–96.
(5) Huang, S.; Liu, S.; Li, J.; Zhao, N.; Wie, W.; Sun, Y. Modified Zinc Oxide for the Direct Synthesis of Propylene Carbonate from Propylene Glycol and Carbon dioxide. *Catal. Lett.* **2007**, *118*, 290–294.
(6) Vrouwenvelder, C. L. M. Separation Method. WIPO Patent Application WO 02/098829, 2002.
(7) Fischer, R.; Stops, P.; Brunner, E.; Weigand, R. Method of separating γ-Butyrolactone from mixtures containing Diethyl Succinate. U.S. Patent 5030328, 1991.
(8) Zhang, D.; Yin, H.; Ge, C.; Xue, J.; Jiang, T.; Yu, L.; Shen, Y. Selective hydrogenation of maleic anhydride to γ-butyrolactone and tetrahydrofuran by Cu-Zn-Zr catalyst in the presence of ethanol. *J. Ind. Eng. Chem.* **2009**, *15*, 537–543.
(9) Vaidya, S. H.; Rode, C. V.; Chaudhari, R. V. Bimetallic Pt-Sn/γ-alumina catalyst for highly selective liquid phase hydrogenation of diethyl succinate to γ-butyrolactone. *Catal. Commun.* **2007**, *8*, 340–344.
(10) Cybulski, A.; Chrzaszcz, J.; Twigg, M. V. Hydrogenation of dimethyl succinate over monolithic catalysts. *Catal. Today* **2001**, *69*, 241–245.
(11) George, E. H.; Norman, H.; Davy, M. L. Process for the Production of Gamma-Butyrolactone. U.S. Patent 4767869, 1988.
(12) Kim, J. I.; Choi, Y. Y.; Park, S. J. Solid-Liquid Equilibria, Excess Molar Volumes, and Molar Refractivity Deviations for Extractive Solvents of Molybdenum. *J. Chem. Eng. Data* **2010**, *55*, 1179–1185.
(13) Barthel, J.; Neueder, R.; Rawytsch, P.; Roch, H. Conductivity study on lithium bromide in propylene Carbonate + acetonitrile mixtures in dilute solutions from 35 to 75°C. *J. Electroanal. Chem.* **1999**, *471*, 78–87.
(14) Yang, S. K. Excess volumes and densities of binary mixtures of γ-butyrolactone+1, 3, 5-trimethylbenzene or 1, 2, 4-trimethylbenzene at several temperatures. *J. Mol. Liq.* **2008**, *140*, 45–47.
(15) Dvid, R. L.; *CRC Handbook of Chemistry and Physics, Internet Version*; CRC Press: Boca Raton, FL, 2005.
(16) Aminabhavi, T. M.; Phayde, H. T. S.; Khinnavar, R. S.; Gopalakrishna, B. Densities, Refractive Indices, Speeds of Sound, and Shear Viscosities of Diethylene Glycol Dimethyl Ether with Ethyl Acetate, Methyl Benzoate, Ethyl Benzoate, and Diethyl Succinate in the Temperature Range from 298.15 to 318.15 K. *J. Chem. Eng. Data* **1994**, *39*, 251–260.
(17) Muhuri, P. K.; Das, B.; Hazra, D. K. Viscosities and Excess Molar Volumes of Binary Mixtures of Propylene Carbonate with Tetrahydrofuran and Methanol at Different Temperatures. *J. Chem. Eng. Data* **1996**, *41*, 1473–1476.
(18) Lu, H.; Wang, J.; Zhao, Y.; Xuan, X.; Zhuo, K. Excess Molar Volumes and Viscosities for Binary Mixtures of γ-Butyrolactone with Methyl Formate, Ethyl Formate, Methyl Acetate, Ethyl Acetate, and Acetonitrile at 298.15 K. *J. Chem. Eng. Data* **2001**, *46*, 631–634.
(19) Korosi, A.; Fabuss, B. M. Viscosity of Liquid Water from 25° to 150° C Measurements in Pressurized Glass Capillary Viscometer. *Anal. Chem.* **1968**, *40*, 157–162.
(20) Han, K. J.; Hwang, I. C.; Park, S. J.; Choi, M. J.; Lee, S. B.; Han, J. S. Vapor-liquid equilibrium, densities and viscosities for the binary system exo-and endo-tetrahydrodicyclopentadiene and pure component vapor pressures. *Fluid Phase Equilib.* **2006**, *249*, 187–191.
(21) Wilson, G. M. Vapor-liquid equilibrium. XI. A new expression for the excess free energy of mixing. *J. Am. Chem. Soc.* **1964**, *86*, 127–130.
(22) Park, S. J.; Han, K. J.; Gmehling, J. Vapor-liquid equilibria and excess properties for methyl tert-butyl ether (MTBE) containing binary systems. *Fluid Phase Equilib.* **2002**, *200*, 399–409.
(23) Stephan, K.; Mayinger, F. *Thermodynamik - Grundlagen und technische Anwendungen.* Berlin, 1992.
(24) Dortmund Data Bank Software Package (DDBSP), version 2006 professional. http://www.ddbst.de.
(25) Perron, G.; Couture, L.; Lambert, D.; Desnoyers, J. E. Phase diagrams, molar volumes, heat capacities, conductivities and viscosities of some lithium salts in aprotic solvents. *J. Electroanal. Chem.* **1993**, *355*, 277–269.
(26) Vijaya Kumar Naidu, B.; Chowdoji Rao, K.; Subha, M. C. S. Densities and Viscosities of Mixtures of Some Glycols and Polyglycols in Dimethyl Sulfoxide at 308.15 K. *J. Chem. Eng. Data* **2002**, *47*, 379–382.
(27) Wankhede, D.; Nilesh, W.; Lande, M.; Arbad, B. Densities and viscosities of propylene carbonate with aromatic hydrocarbons (benzene, 1,4-dimethylbenzene and ethylbenzene) at 288.15, 298.15 and 308.15 K. *Phys. Chem. Liq.* **2008**, *46*, 319–327.

Received for review August 19, 2010. Accepted November 30, 2010.

JE100803E